Experimental section

General experimental considerations. DNA oligonucleotides were prepared by solid-phase synthesis at IDT (Coralville, IA). RNA transcripts were prepared by in vitro transcription using T7 RNA polymerase and a double-stranded DNA template prepared by annealing two synthetic DNA oligonucleotides.[1] DNA oligonucleotides and RNA transcripts were purified by denaturing PAGE using 1× TBE running buffer (89 mM each Tris and boric acid, 2 mM EDTA, pH 8.3). Samples were eluted from the gel by the crush-and-soak method in 10 mM Tris pH 8.0, 1 mM EDTA, 300 mM NaCl (TEN) buffer, recovered by ethanol precipitation, and quantified by UV absorbance.

Kinetic studies – general considerations. The ligation abilities of 10DM24 and the engineered constructs were tested using the short RNA sequences originally used for selection of 10DM24.[2] The sequence of the L RNA substrate (Fig. 1) was 5′-GGAUAAUACGACUCACUAUA-3′, with the branch-site adenosine underlined. The L RNA substrate was 5′ end radiolabeled with γ-^{32}P-ATP and T4 polynucleotide kinase. The R RNA substrate was an RNA transcript to provide the 5′-triphosphate necessary for the ligation reaction (Fig. 1). The sequence of the R substrate was 5′-GGAAGAGAUGGCGACGG-3′. All assays were conducted under conditions similar to those previously reported for studies of 10DM24.[2-3] Prior to initiating the reaction, appropriate oligonucleotides were annealed in 5 mM HEPES (pH 7.5), 15 mM NaCl, and 0.1 mM EDTA by heating at 95 °C for 3 min and cooling on ice for 5 min. The reaction buffer, $MgCl_2$, and ATP (for designated reactions) were then added to initiate the reactions. Final incubation conditions were 50 mM CHES (pH 9.0), 150 mM NaCl, 2 mM KCl, 40 mM $MgCl_2$, and ATP at 25 °C or 37 °C as indicated in figure legends. At appropriate time points, 1.5 μL was removed from each reaction and quenched into 8 μL stop solution (80% formamide, 1× TB [89 mM each Tris and boric acid, pH 8.3], 50 mM EDTA, 0.025% bromophenol blue and 0.025% xylene cyanol). Samples were separated by 20% denaturing PAGE and imaged using a PhosphorImager (GE Healthcare, Piscataway, NJ). Gel images were analyzed using Quantity One (Bio-Rad, Hercules, CA) and the data were fit using KaleidaGraph (Synergy Software, Reading, PA) to first-order kinetics using yield = $Y•(1–e^{–kt})$, where $k = k_{obs}$ and Y = final yield. When ligation yields had not leveled off at the final time point, k_{obs} was determined from the slope of the linear fit of the data.

Assays to identify suitable insertion sites. Potential insertion sites in the two enzyme loops of 10DM24 (designated loop A and loop B) for the ATP aptamer sequence were investigated using two different inserts. The sequence of the hairpin insertion was 5′-ACGTTCGAAAGAACGT-3′, with the complementary regions underlined, and the sequence of the unstructured insert was 5′-CAACAACAACAACAA-3′. The sequences of all deoxyribozyme constructs are provided in Table S1. Kinetic assays were conducted as described above using the previously described trimolecular format.[2-3] The ratio of 5′ end radiolabeled L substrate (*L) to deoxyribozyme (E) to R substrate (R) was 1:5:10, where the concentration of deoxyribozyme was 0.5 μM. This ratio was used to ensure all of *L is bound to a deoxyribozyme and that all *L-E complexes are bound to R. Other ratios that maintain *L < E < R could also be used. Reactions proceeded at 37 °C for up to 2 h. Samples were separated by 20% denaturing PAGE and analyzed as described above.

Assays with aptamer-modified deoxyribozymes. Assays involving deoxyribozyme constructs that contained the ATP aptamer sequence[4] as shown in Fig. 1 were conducted in the trimolecular

Supplementary Material (ESI) for Chemical Communications

format. The ratio of *L:E:R was 1:5:10 where the concentration of deoxyribozyme (E) was 0.25 μM. Reactions proceeded at either 25 °C or 37 °C for up to 2 h. For constructs involving the splitzymes, the ratio of 5′ end radiolabeled L substrate (*L) to L deoxyribozyme (base pairing primarily to the L RNA substrate) to R deoxyribozyme (base pairing primarily to the R RNA substrate) to R substrate was 1:2.5:5:10, where the concentration of the R deoxyribozyme was 0.25 μM. Reactions with splitzymes proceeded at 25 °C or 37 °C as indicated in the figure legends.

ATP concentration assays. Assays investigating the ATP concentration dependence utilized the 4 bp stem aptazyme construct in the trimolecular format. The ratio of *L:E:R was 1:5:10 where the concentration of deoxyribozyme (E) was 0.25 μM. Reactions proceeded at 25 °C or 37 °C for up to 2 h. Samples were separated by 20% denaturing PAGE and analyzed as described above. The average yields at the 2 h time point were fit to the Hill equation as described[5] using the equation $yield=y_0+(Y_{max}*x^n/(C_{0.5}^n+x^n))$, where y_0 is the initial yield, Y_{max} is the maximum yield, $C_{0.5}$ is the equilibrium concentration at half saturation, and n is the Hill coefficient. Data was fit using a Hill coefficient of 2.

Insertion site assessment

The ATP aptamer contains a closing 4 bp stem that is stabilized when ATP binds the aptamer.[6] In our construct, this stem is placed near the enzyme loop of the deoxyribozyme. We designed a hairpin loop with a 6 bp stem and a stable GAAA tetraloop. This structured insert allowed us to identify insertion sites that may accept the aptamer-ligand complex while maintaining deoxyribozyme catalytic activity. We also tested an unstructured insert consisting of CAA repeats to identify locations where an unstructured insert mimicking the aptamer without its ligand shows reduced ligation activity. Insertion sites that tolerate the structured insert but show reduced ligation activity with the unstructured insert represent candidate locations for the ATP aptamer that may produce an ATP-upregulated aptazyme.

We identified several locations in the enzyme loops of 10DM24 for evaluating sequence insertion (Fig. S1a). Of the four tested locations, two sites (A1 and B) tolerated the inserts. For these sites, ligation activity with the hairpin insert was comparable to the unmodified 10DM24 (Fig. S1b). However, site A1 also tolerated the unstructured insert with ligation activity essentially identical to unmodified 10DM24. The unstructured insert was less tolerated at site B, with a 4-fold decrease in k_{obs} (Fig. S1b). Ligation activity with the unstructured insert indicates that the deoxyribozyme can loop out the unstructured nucleotides in these locations and still form a catalytically competent structure. Addition of an oligonucleotide complementary to the CAA inserts at site A1, resulting in a double-stranded region, suppressed ligation activity from 95% to only ~6% in 2 h (data not shown). This result indicates that a structured insert that does not allow the enzyme region ends flanking the insert to come close together, at least at site A1, is detrimental to deoxyribozyme activity. Site A2 did not tolerate either insert very well. Site A3 unexpectedly tolerated the unstructured insert but showed very little activity with the hairpin insert. The interference from the hairpin insert at site A3 is possibly due to the formation of an additional base pair between the C and the G of the enzyme region flanking the insertion site (Fig. S1a), which would make those nucleotides unavailable for other interactions important for catalysis.

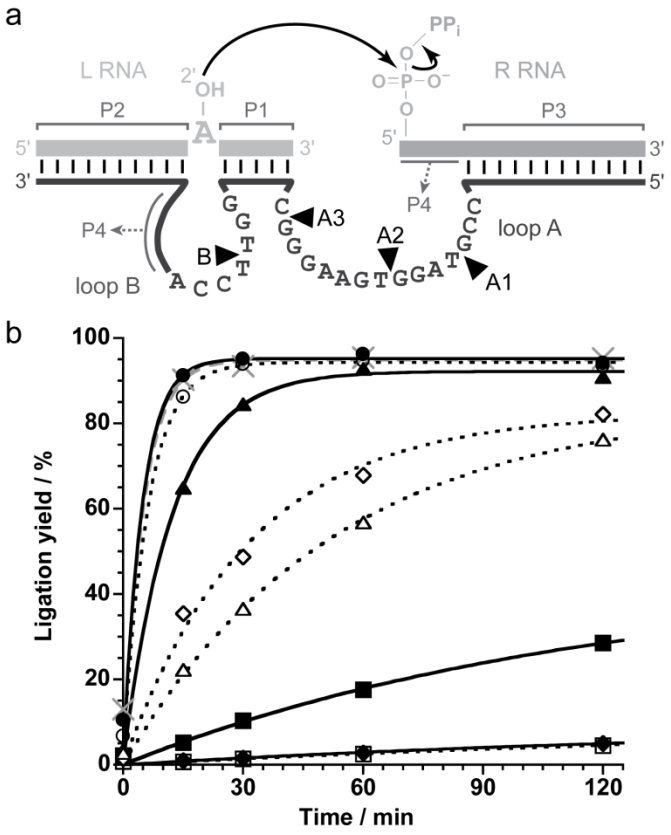

Fig. S1. Potential insertion sites for the ATP aptamer in 10DM24 enzyme loops and ligation activity of 10DM24 constructs. (a) The 10DM24 deoxyribozyme[2] and its two RNA substrates. The four sites chosen for insertion studies are indicated with arrowheads. (b) Ligation assays for 10DM24 constructs. Assays were conducted using 50 mM CHES (pH 9.0), 150 mM NaCl, 2 mM KCl, and 40 mM $MgCl_2$ at 37 °C. 10DM24 (grey crosses) served as a positive control. Hairpin insert (solid markers) and unstructured insert (open markers) were tested at sites A1 (circles), A2 (squares), A3 (diamonds), and B (triangles). Data was fit to first-order kinetics as described in the Experimental Section.

Additional site B results

Additional studies with the aptamer inserted into site B were conducted at 25 °C. These studies are directly analogous to the studies shown in Fig. 2, except for the change in reaction temperature. 25 °C was the temperature used in the selection of the ATP aptamer[4] and would be a useful temperature for sensor applications. Aptazyme activity was modulated by ATP addition for all stem lengths (Fig. S2a). However, the rates and yields with added ATP are lower at 25 °C compared to 37 °C (Fig. S2c). There was also no increase in the activation factor between reactions without ATP and with ATP at 25 °C versus 37 °C.

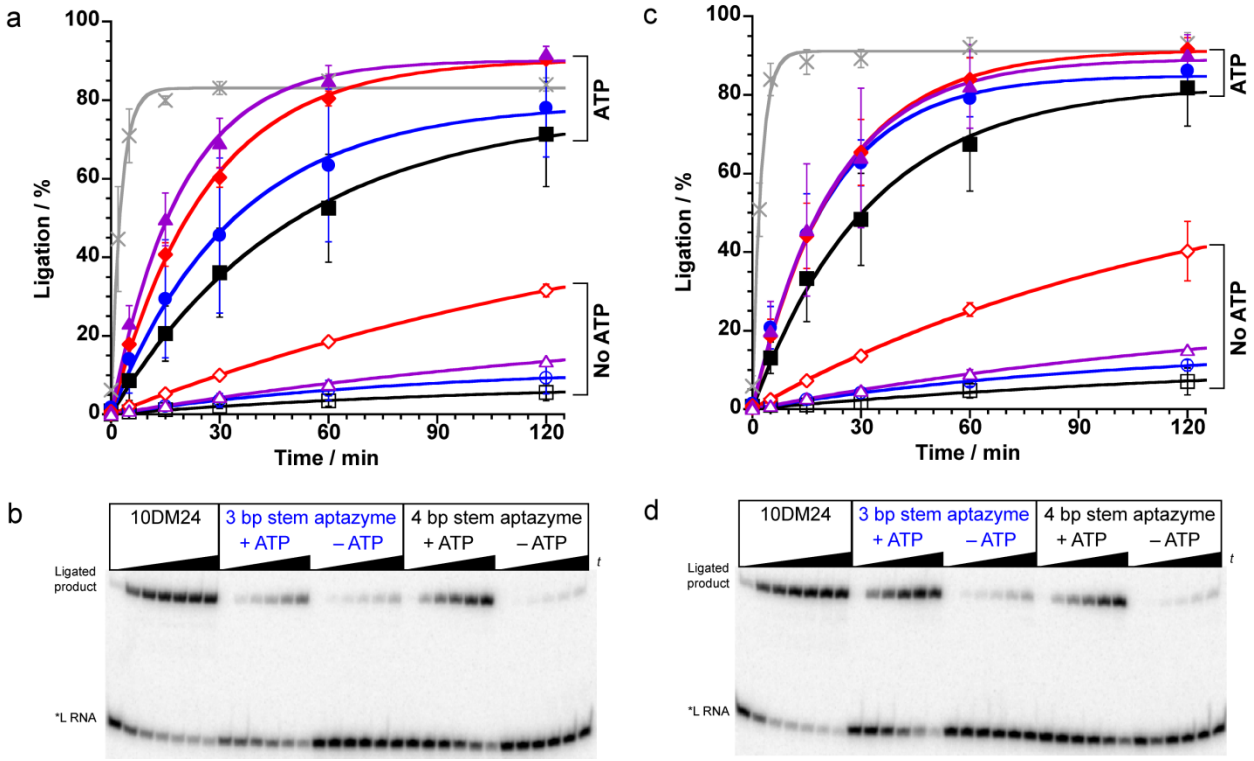

Fig. S2. Investigation of stem length dependence for 10DM24 aptazyme constructs at 25 °C and 37 °C. (a) 10DM24 was modified with the ATP aptamer in loop B as shown in Fig. 1 to create an aptazyme. Assays were conducted using 50 mM CHES (pH 9.0), 150 mM NaCl, 2 mM KCl, and 40 mM $MgCl_2$ in the presence (solid symbols) or absence (open symbols) of 5 mM ATP at 25 °C. Constructs contained the 4 bp stem (black squares), the 3 bp stem (blue circles), the 2 bp stem (red diamonds), or the 1 bp stem (purple triangles). Unmodified 10DM24 in the absence of ATP is shown as grey crosses; inclusion of ATP had no effect on the reaction (data not shown). The sequences of the deoxyribozymes are provided in Table S1. Each data point represents the average ligation yield at the indicated time point for at least two independent trials. Error bars for data points with three or more trials represent the standard deviation, while error bars for data points with two trials represent the data range. Data was analyzed and fit as described in the Experimental Section. k_{obs} and final % yields are provided in Table S2. (b) Representative PAGE of results at 25 °C. Unmodified 10DM24 served as a positive control. Time points were taken at 0, 2 (for 10DM24), 5, 15, 30, 60, and 120 min. Products were separated by 20% denaturing PAGE. (c) Results at 37 °C. Data from Fig. 2 is represented here in color for direct comparison with data from 25 °C assays. (d) Representative PAGE of results at 37 °C.

When 10DM24 was split at site B and the ATP aptamer halves were replaced with sequences that could base pair and form a 12 bp stem, the ligation activity was high, although merely splitting the enzyme region in this fashion did reduce the reaction rate (Fig. S3a). The ligation activity was dependent on the two halves being able to come together and interact. When the sequences were unable to base pair, the ligation activity dropped to levels observed when no ATP was present for the aptazyme constructs.

When the site B splitzymes modified with the ATP aptamer halves were assayed at 25 °C, there was little difference in rate or final yield for the splitzymes at 25 °C (Fig. S3b) versus 37 °C (Figure S3c). However, substantial ligation activity was observed at 25 °C when no ATP was added to the reaction (Figure S3b). The lower reaction temperature may stabilize weak interactions between the aptamer halves, resulting in ligation activity in the absence of ATP.

Supplementary Material (ESI) for Chemical Communications

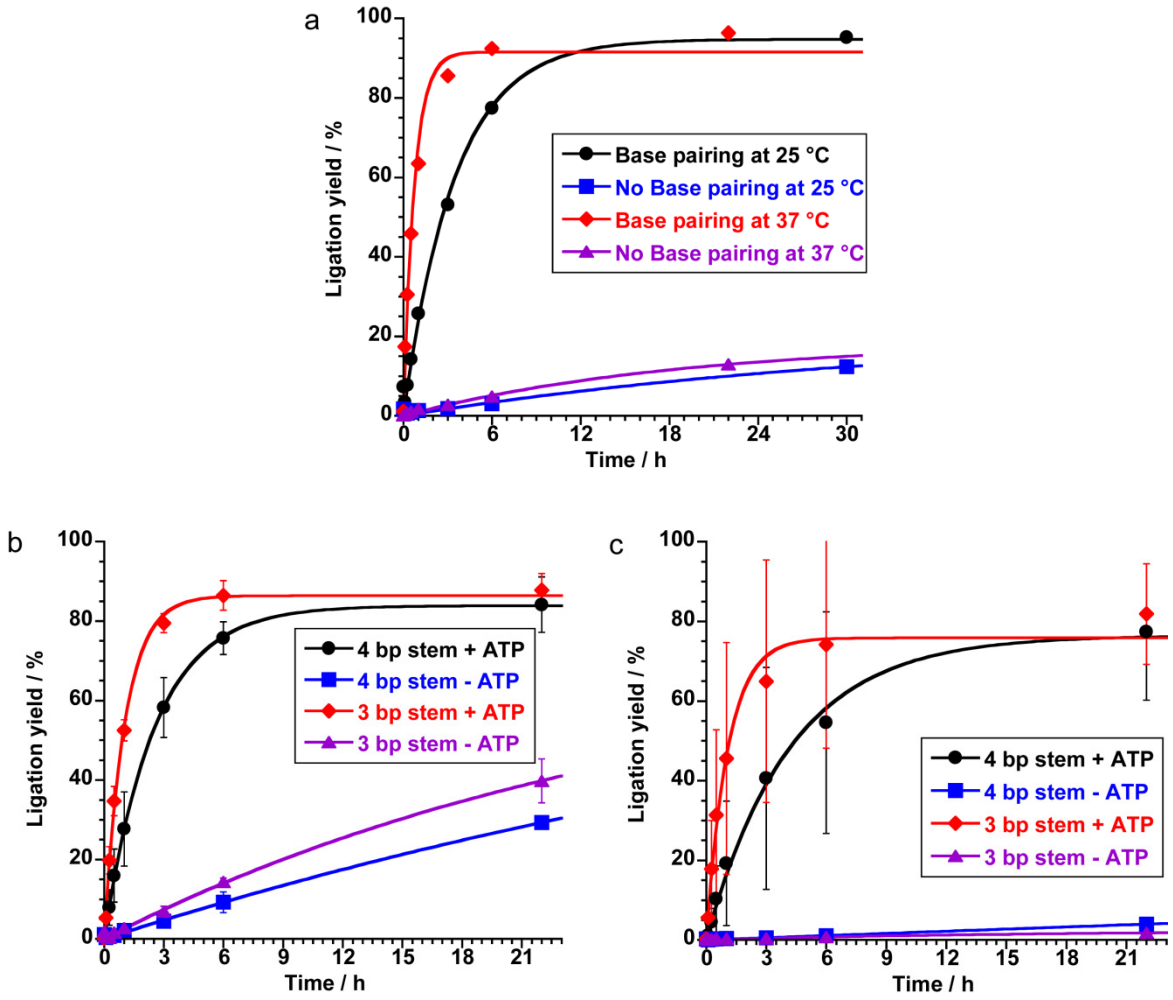

Figure S3. Ligation activity for site B splitzymes. (a) Studies conducted using enzyme halves that can be brought together via a 12 bp interaction ("base pairing") or with enzyme halves unable to base pair ("no base pairing"). Assays were conducted using 50 mM CHES (pH 9.0), 150 mM NaCl, 2 mM KCl, and 40 mM $MgCl_2$ at 25 °C or 37 °C. Data was fit as described in the Experimental Section. k_{obs} was 0.3 h^{-1} at 25 °C (black) and 1.4 h^{-1} at 37 °C (red) for the base pairing construct versus 0.004 h^{-1} at 25 °C (blue) and 0.006 h^{-1} at 37 °C (purple) for the no base pairing construct. (b) Splitzyme constructs where 10DM24 was split in loop B and modified with the ATP aptamer as shown in Fig. 1 to create a splitzyme. Assays were conducted as above in the presence or absence of 5 mM ATP at 25 °C. Constructs contained either the 4 bp stem or the 3 bp stem adjacent to loop B. Each data point represents the average ligation yield at the indicated time point for at least two independent trials. Error bars for data points with three or more trials represent the standard deviation, while error bars for data points with two trials represent the data range. Data was analyzed and fit as described in the Experimental Section. k_{obs} and final % yields are provided in Table S3. (c) Splitzyme constructs tested and analyzed under the same conditions as (b) except at 37 °C.

Specificity for adenosine and its phosphorylated forms ATP, ADP, and AMP

The specificity of aptazyme modulation was tested by including 5 mM of GTP, CTP, or UTP in the reactions in place of ATP. Inclusion of GTP, CTP, or UTP resulted in ligation yields comparable to reactions with no ATP (Fig. S4a). These results were compared to reactions which included 5 mM of ATP, ADP, AMP, or adenosine. Adenosine and its phosphorylated forms all produced high ligation yields (Fig. S4a). Ligation activity in the presence of ATP, ADP, AMP,

and adenosine was expected because the Huizenga and Szostak aptamer has been shown to bind adenosine, ATP, and AMP with similar affinities.[4] The splitzyme construct showed the same specificity for adenosine and its phosphorylated forms over GTP, CTP, and UTP (Fig. S4b).

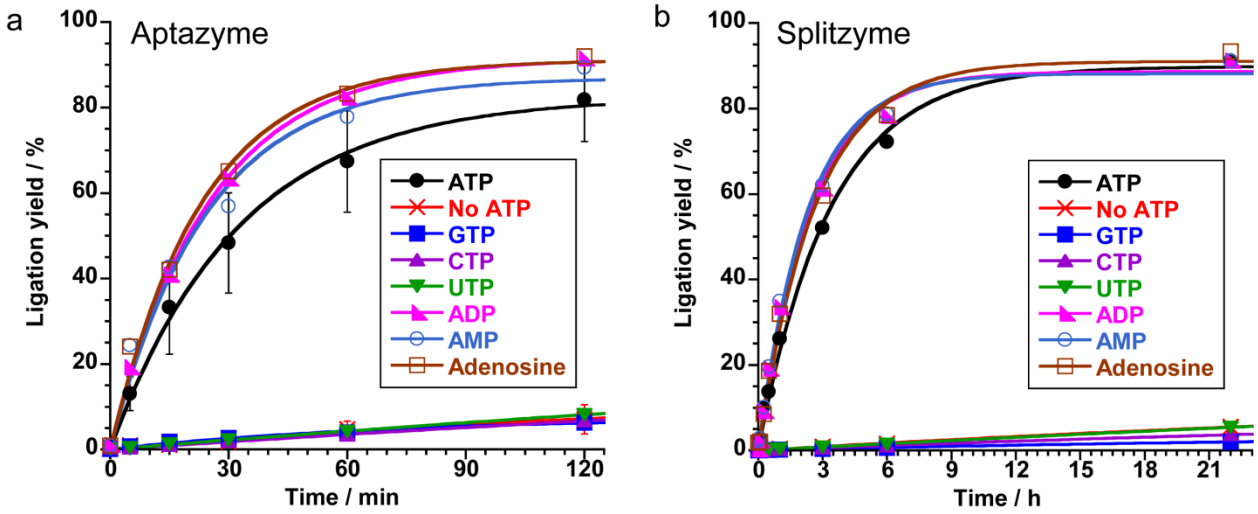

Fig. S4. Ligation activity in the presence of each standard NTP, ADP, AMP, and adenosine. (a) Studies conducted with the aptazyme construct. Assays were conducted using 50 mM CHES (pH 9.0), 150 mM NaCl, 2 mM KCl, 40 mM $MgCl_2$, and 5 mM of the indicated nucleotide at 37 °C. (b) Studies conducted with the splitzyme construct. Assays were conducted as in (a). Data was fit as described in the Experimental Section.

ATP Concentration Experiments

Using the 4 bp stem aptazyme construct, we investigated the ATP concentration dependence over a wide range of added ATP concentrations at 25 °C and 37 °C (Fig. S5). Maximum yields were obtained around 500 μM ATP. At 25 °C, modest inhibition of ligation was observed at 5 mM ATP, with greater inhibition at 10 mM ATP (Figure S5a). At 37 °C, the inhibition was only prominent at 10 mM added ATP (Figure S5b). The inhibition was attributed to chelation of Mg^{2+} by ATP based on results of previous studies with 10DM24 in the presence of high concentrations of NTPs.[7] Addition of higher concentrations of ATP reduces the amount of Mg^{2+} available to the deoxyribozyme. Plotting the final % yield data from the 25 °C assays using a Hill coefficient of 2 resulted in an apparent K_d for ATP of 81 ± 48 μM (Figure S5c), which is equivalent within error to the value of 82 ± 27 μM at 37 °C (Figure S5d).

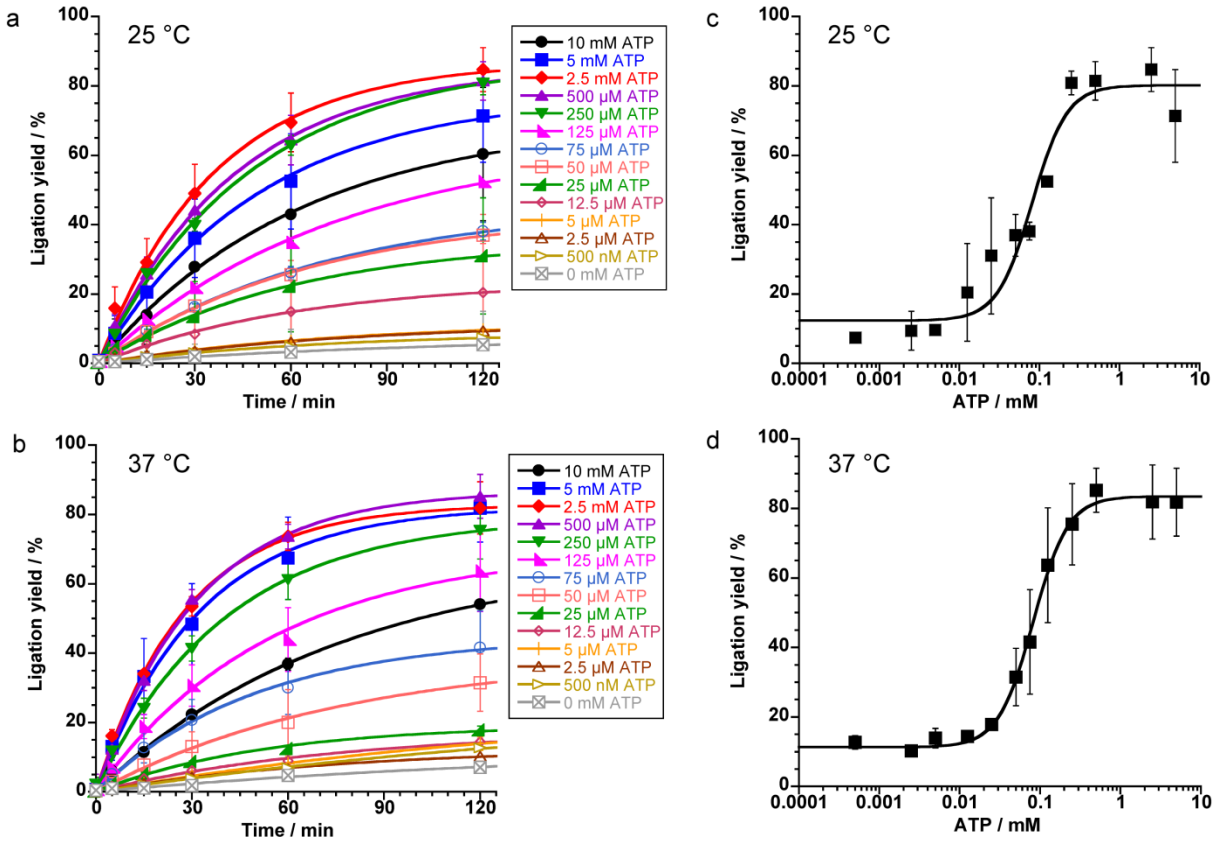

Fig. S5. ATP concentration studies. (a) Assays were conducted at 25 °C using the 4 bp stem aptazyme construct. Reaction conditions included 50 mM CHES (pH 9.0), 150 mM NaCl, 2 mM KCl, 40 mM $MgCl_2$, and the indicated concentration of ATP at 25 °C. (b) Assays conducted at 37 °C under the same reaction conditions as in (a). Each data point represents the average ligation yield at the indicated time point for at least two independent trials. Error bars for data points with three or more trials represent the standard deviation, while error bars for data points with two trials represent the data range. Data was analyzed and fit as described in the Experimental Section. (c) Hill plot of assays conducted at 25 °C. Each data point represents the average ligation yield at the 120 min time point for at least two independent trials. The data was fit using a Hill coefficient of 2. (d) Hill plot of assays conducted at 37 °C.

Table S1. Sequences of Deoxyribozyme Constructs

DNA Sequence[a]	Description[b]
CCGTCGCCATCTCCCGTAGGTGAAGGGCGTGAGGGTTCCATTCCCGTATTATCC	10DM24[2]
CCGTCGCCATCTCCCGACGTTCGAAAGAACGTTAGGTGAAGGGCGTGAGGGTTCCATTCCCGTATTATCC	Hairpin insert, site A1
CCGTCGCCATCTCCCGCAACAACAACAACAATAGGTGAAGGGCGTGAGGGTTCCATTCCCGTATTATCC	Unstructured insert, site A1
CCGTCGCCATCTCCCGTAGGACGTTCGAAAGAACGTTGAAGGGCGTGAGGGTTCCATTCCCGTATTATCC	Hairpin insert, site A2
CCGTCGCCATCTCCCGTAGGCAACAACAACAACAATGAAGGGCGTGAGGGTTCCATTCCCGTATTATCC	Unstructured insert, site A2
CCGTCGCCATCTCCCGTAGGTGAAGGGACGTTCGAAAGAACGTCGTGAGGGTTCCATTCCCGTATTATCC	Hairpin insert, site A3
CCGTCGCCATCTCCCGTAGGTGAAGGGCAACAACAACAACAACGTGAGGGTTCCATTCCCGTATTATCC	Unstructured insert, site A3
CCGTCGCCATCTCCCGTAGGTGAAGGGCGTGAGGGTACGTTCGAAAGAACGTTCCATTCCCGTATTATCC	Hairpin insert, site B
CCGTCGCCATCTCCCGTAGGTGAAGGGCGTGAGGGTCAACAACAACAACAATCCATTCCCGTATTATCC	Unstructured insert, site B
CCGTCGCCATCTCCCGTAGGTGAAGGGCGTGAGGGTACCTGGGGGAGTATTGCGGAGGAAGGTTCCATTCCCGTATTATCC	ATP aptamer, 4 bp stem, site B
CCGTCGCCATCTCCCGTAGGTGAAGGGCGTGAGGGTACTGGGGGAGTATTGCGGAGGAAGTTCCATTCCCGTATTATCC	ATP aptamer, 3 bp stem, site B
CCGTCGCCATCTCCCGTAGGTGAAGGGCGTGAGGGTATGGGGGAGTATTGCGGAGGAATTCCATTCCCGTATTATCC	ATP aptamer, 2 bp stem, site B
CCGTCGCCATCTCCCGTAGGTGAAGGGCGTGAGGGTTGGGGGAGTATTGCGGAGGAATCCATTCCCGTATTATCC	ATP aptamer, 1 bp stem, site B
CCGTCGCCATCTCCCGTAGGTGAAGGGCGTGAGGGTTCGTTCAGCTCG	Splitzyme R side, base pairing, site B
CGAGCTGAACGATCCATTCCCGTATTATCC	Splitzyme L side, base pairing, site B
CCGTCGCCATCTCCCGTAGGTGAAGGGCGTGAGGGTCAACAACAACAA	Splitzyme R side, no base pairing, site B
CAACAACAACAATCCATTCCCGTATTATCC	Splitzyme L side, no base pairing, site B
CCGTCGCCATCTCCCGTAGGTGAAGGGCGTGAGGGTACCTGGGGGAGTA	Splitzyme R side, ATP aptamer 4 bp stem, site B
TACGGAGGAAGGTTCCATTCCCGTATTATCC	Splitzyme L side, ATP aptamer 4 bp stem, site B
CCGTCGCCATCTCCCGTAGGTGAAGGGCGTGAGGGTACTGGGGGAGTA	Splitzyme R side, ATP aptamer 3 bp stem, site B
TACGGAGGAAGTTCCATTCCCGTATTATCC	Splitzyme L side, ATP aptamer 3 bp stem, site B

[a] DNA sequences are shown 5′→3′, with the enzyme loop regions underlined and the insertions in red. The first underlined region is loop A and the second underlined region is loop B. [b] R side refers to the deoxyribozyme half that base pairs primarily to the R RNA substrate, while L side refers to the deoxyribozyme half that base pairs primarily to the L RNA substrate.

Table S2. Observed rate constants for aptazyme constructs[a]

Aptazyme Construct	5 mM ATP 25 °C		0 mM ATP 25 °C		5 mM ATP 37 °C		0 mM ATP 37 °C	
	k_{obs}	% Yield	k_{obs}	% Yield	k_{obs}	% Yield	k_{obs}	% Yield
4 bp stem	0.02	71	0.0006	6	0.03	82	0.0006	7
3 bp stem	0.03	78	0.001	9	0.05	86	0.001	11
2 bp stem	0.04	90	0.003	32	0.04	92	0.004	40
1 bp stem	0.05	92	0.002	14	0.05	90	0.002	15

[a] Units for rate constants are min^{-1} and the % yield is the average final % yield.

Table S3. Observed rate constants for splitzyme constructs[a]

Splitzyme Construct	5 mM ATP 25 °C		0 mM ATP 25 °C		5 mM ATP 37 °C		0 mM ATP 37 °C	
	k_{obs}	% Yield	k_{obs}	% Yield	k_{obs}	% Yield	k_{obs}	% Yield
4 bp stem	0.40	84	0.01	29	0.24	77	0.002	4
3 bp stem	0.96	88	0.02	40	0.87	69	0.0008	2

[a] Units for rate constants are h^{-1} and the % yield is the average final % yield.

Table S4. Observed rate constants for ATP concentrations studies[a]

ATP concentration	25 °C		37 °C	
	k_{obs}	% Yield	k_{obs}	% Yield
10 mM	0.016	60	0.013	54
5 mM	0.020	71	0.031	82
2.5 mM	0.028	85	0.036	82
500 μM	0.024	81	0.032	85
250 μM	0.021	81	0.025	75
125 μM	0.008	52	0.018	64
75 μM	0.0062	38	0.012	42
50 μM	0.0054	37	0.0048	32
25 μM	0.0035	31	0.0028	18
12.5 μM	0.0023	20	0.0023	14
5 μM	0.0011	10	0.0015	14
2.5 μM	0.0010	9	0.0016	10
500 nM	0.0008	7	0.0013	13
0 mM	0.0005	5	0.0006	7

[a] Units for rate constants are min^{-1} and the % yield is the average final % yield.

REFERENCES

1. J. F. Milligan, D. R. Groebe, G. W. Witherell and O. C. Uhlenbeck, *Nucleic Acids Res.*, 1987, **15**, 8783-8798.
2. E. Zelin, Y. Wang and S. K. Silverman, *Biochemistry*, 2006, **45**, 2767-2771.
3. D. A. Baum and S. K. Silverman, *Angew. Chem. Int. Ed.*, 2007, **46**, 3502-3504.
4. D. E. Huizenga and J. W. Szostak, *Biochemistry*, 1995, **34**, 656-665.
5. M. Levy and A. D. Ellington, *Chem. Biol.*, 2002, **9**, 417-426.
6. C. H. Lin and D. J. Patel, *Chem. Biol.*, 1997, **4**, 817-832.
7. C. Höbartner and S. K. Silverman, *Angew. Chem. Int. Ed.*, 2007, **46**, 7420-7424.